Harnessing thermal waves for heat pumping

Jose Ordonez-Miranda,[1,2,*] Roman Anufriev,[1,3] Masahiro Nomura,[1,2] and Sebastian Volz[1,2]

[1] *LIMMS, CNRS-IIS IRL 2820, The University of Tokyo, Tokyo 153-8505, Japan*
[2] *Institute of Industrial Science, The University of Tokyo, Tokyo 153-8505, Japan*
[3] *Univ. Lyon, INSA Lyon, CNRS, CETHIL, UMR5008, 69621 Villeurbanne, France*

(Received 17 March 2024; revised 23 April 2024; accepted 3 May 2024; published 20 May 2024)

Based on the nonlinear propagation of thermal diffusion waves, we demonstrate the existence of a net heat current even in the absence of a mean temperature gradient. Unlike the steady-state heat current, this current of thermal waves is not driven by the material thermal conductivity, but rather by its temperature derivative. The heat current propagates outward or inward of its excitation source when the thermal conductivity increases or decreases with temperature, respectively. The modulation of the heat flux direction can thus be achieved by varying the material temperature around the thermal conductivity peak exhibited by various dielectrics. For a silicon plate with a thermal conductivity peak at 40 K that supports the propagation of thermal waves with an excitation amplitude of 10 K, we observe a net heat flux exceeding 60 W cm^{-2} at 20 K and falling below −20 W cm^{-2} at 65 K. Larger excitation amplitudes allow higher or lower heat fluxes to be achieved, which makes them easy to observe and potentially apply for harvesting or evacuating thermal energy in systems undergoing natural temperature fluctuations on earth and in outer space.

DOI: 10.1103/PhysRevApplied.21.054037

I. INTRODUCTION

Thermal diffusion waves are temperature fluctuations that drive many physical phenomena, including heat conduction and thermal imaging in solids, liquids, and gases. These temperature oscillations form the basis for probing the properties of materials via several measurement techniques [1–8]. The propagation of these peculiar waves is determined by a first-order time derivative of temperature only and they are generated by the transfer of kinetic energy from hot to cold regions through atomic collisions. These waves are usually excited with thermal, optical, and electrical sources periodically modulated in time with a given frequency. As this modulation frequency increases, the waves' propagation distance decreases [9], which allows materials to be probed at different depth positions. However, the average heat flux of the thermal waves over one oscillation period is zero, as established by Fourier's law of heat diffusion [10]. Therefore, unlike electromagnetic or acoustic waves, the thermal waves do not carry energy, which avoids their application as effective heat carriers. This zero-energy propagation arises in materials with constant thermal properties and could be overcome in nonlinear media [11].

Nonlinear heat conduction driven by a temperature-dependent thermal conductivity is of primary importance to efficiently control heat currents [12–14]. Given that the generation, transport, and utilization of the global energy involves the loss of around 70% in the form of waste heat that is mainly released into the environment [15], this heat control can help optimize the energy consumption [16]. The temperature dependence of the thermal conductivity generates an asymmetric material response that has been used to develop thermal analogs of electronic devices, such as thermal diodes [4,17–21], thermal transistors [22,23], thermal logic gates [24], thermal memories [25], and thermal memristors [26,27]. Based on the asymmetric temperature variations of the thermal conductivities of two materials, Shen *et al.* [28] developed a temperature-trapping theory and proposed an energy-free thermostat able to self-maintain a desired constant temperature without consuming energy. More recently, Wang *et al.* [29] introduced thermoelectric effects in this theory and proposed a negative-energy thermostat capable of generating electricity from a constant ambient temperature. These conceptions of thermal devices thus capitalize on the nonlinear heat conduction under steady-state conditions and do not consider the natural and daily temperature fluctuations of the environment. In fact, until now, very few works have tackled the nonlinear heat conduction periodically modulated in time [30–32]. By exciting a nonlinear asymmetric lattice with a temperature difference oscillating with time,

*Corresponding author: jose.ordonez@cnrs.fr, ordonez@iis.u-tokyo.ac.jp

the appearance of a net heat current was predicted in the absence of an average thermal bias [33–35]. This net heat flux was also obtained by exploiting the metal-insulator transition of a VO_2 ribbon supporting the propagation of thermal diffusion waves [11,36,37]. The temperature oscillations have also been applied to generate exotic effects, such as the reciprocity of thermal diffusion [38], the configurable phase transitions of a topological material [39], and the rectification of thermal-wave heat currents [40]. Such fine-tuning of dynamical heat fluxes in idealized microscopic nonlinear lattices or phase-change materials with a narrow transition temperature range is also expected to be possible with common and abundant dielectric materials exhibiting significant variations of their thermal conductivity in a wide enough temperature interval. In particular, the competing effects of different scattering mechanisms of phonons in these materials often result in a thermal conductivity peak at a certain temperature. For instance, unlike the monotonic variation of the VO_2 thermal conductivity mainly from 340 to 345 K [11], the thermal conductivity of silicon (Si) peaks at 40 K and exhibits sizable changes for temperatures between 20 and 400 K. As the sign of this thermal conductivity slope changes in the vicinity of its peak, the excitation and propagation of thermal waves in Si and similar dielectrics could lead to the harvesting (pump in) or evacuation (pump out) of heat currents. However, this thermal conductivity peak of various dielectrics has not yet been exploited to tune the magnitude and direction of the net heat flux of thermal waves.

In this work, we theoretically demonstrate the existence of a net heat current generated by thermal waves propagating in a dielectric, even in the absence of a mean temperature gradient. In contrast to the usual steady-state heat conduction, the intensity and direction of this thermal-wave heat current are no longer driven by thermal conductivity, but rather by its temperature derivative. Our quantitative results for a Si plate uncover a nonlinear mechanism of modulated heat diffusion that could be useful to harvest thermal energy from the temperature fluctuations of the environment or systems out of equilibrium.

II. THEORY

Let us consider two thermal baths exchanging heat through conduction via a material of length l, due to their temperature difference $T_h - T_c + \Delta T\cos(\omega t)$ periodically modulated in time t, as shown in Fig. 1. To ensure the material thermalization, we suppose that the modulation period $2\pi/\omega$ is much longer than the material thermalization time (the time required to reach the thermal equilibrium among the material phonons), which is typically shorter than 100 μs, for a broad variety of dielectrics [42]. The thermal conductivity $k(T)$ and volumetric heat capacity $C(T)$ of the material depend strongly on temperature T, as is the case for Si [Fig. 1(b)] and most materials in a large

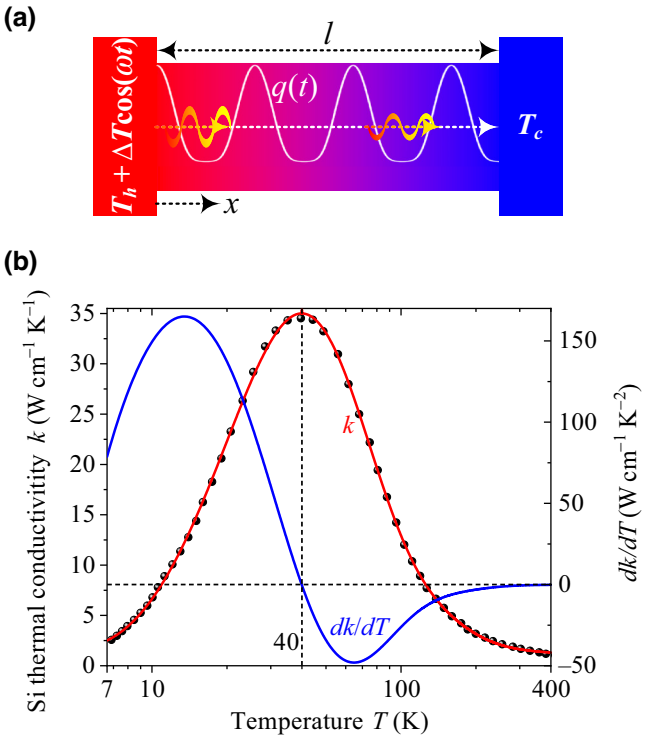

FIG. 1. (a) Scheme of a solid plate supporting heat conduction between two thermal baths due to their temperature difference $T_h - T_c + \Delta T\cos(\omega t)$ periodically modulated in time. The nonsymmetric oscillations of the heat flux q around its steady-state value (dashed white line) generate a net heat flux of thermal waves, whose intensity and direction are represented by the wavy arrows. (b) Si thermal conductivity and its temperature derivative as functions of temperature. The black points on top of the red curve represent experimental values of the thermal conductivity of bulk Si [41].

enough interval of temperatures. Assuming that the system sides at $x = 0$ and l are uniformly heated up by the thermal baths, the one-dimensional heat conduction is characterized by the spatiotemporal distribution of the temperature $T(x,t)$ and heat flux $q(x,t)$ given by the following diffusion equation and Fourier's law, respectively:

$$\frac{\partial}{\partial x}\left(k(T)\frac{\partial T}{\partial x}\right) = C(T)\frac{\partial T}{\partial t}, \tag{1a}$$

$$q = -k(T)\frac{\partial T}{\partial x}. \tag{1b}$$

As illustrated in Fig. 1(a), the temperature is subjected to the boundary conditions $T(0,t) = T_h + \Delta T\cos(\omega t)$ and $T(l,t) = T_c$, with ΔT being the amplitude of the periodic modulation at frequency ω. Equation (1a) does not have an analytical solution for general temperature functions of $k(T)$ and $C(T)$, and therefore its solution should be obtained numerically. However, when the modulation frequency ω is low enough and/or the length l is sufficiently

small, the transient effects can be neglected ($\partial T/\partial t \to 0$) and Eq. (1a) becomes independent of the heat capacity. In this quasisteady regime, the heat flux becomes independent of the position, as established by Eq. (1a). For a material with constant thermal properties (independent of temperature and position), this regime is reached for $\omega \ll 2k/Cl^2$ (thermally thin material) [11]. Considering that the Si thermal diffusivity $\alpha = k/C = 0.8$ and 278.6 cm^2/s at 300 and 40 K [41,43], the quasisteady-state regime in a 5-mm-long Si plate at these temperatures is expected to appear for $\omega \ll 6.4$ and 2230 rad/s, respectively. Under this thermally thin condition used throughout this work, the analytical integration of Eq. (1a) yields

$$ql = \int_{T_c}^{T_h+\Delta T\cos(\omega t)} k(T)dT. \tag{2}$$

The heat flux is thus driven by the temperature dependence of the thermal conductivity inside the interval $[T_c; T_h + \Delta T\cos(\omega t)]$ modulated in time. Considering that the modulation amplitude ΔT is much smaller than its steady-state counterpart ($\Delta T \ll T_h$), the right-hand side of Eq. (2) can be expanded in a Taylor series as follows:

$$\begin{aligned} ql = &\int_{T_c}^{T_h} k(T)dT + \Delta T\cos(\omega t)k(T_h) \\ &+ \frac{[\Delta T\cos(\omega t)]^2}{2!}k'(T_h) \\ &+ \frac{[\Delta T\cos(\omega t)]^3}{3!}k''(T_h) + \ldots. \end{aligned} \tag{3}$$

The average heat flux $\bar{q} = \tau^{-1}\int_0^\tau q(t)dt$ over one period $\tau = 2\pi/\omega$ then becomes independent of frequency ω and is given by

$$\begin{aligned} \bar{q}l = &\int_{T_c}^{T_h} k(T)dT + \left(\frac{\Delta T}{2}\right)^2 k'(T_h) \\ &+ \left(\frac{\Delta T}{2\sqrt{2}}\right)^4 k'''(T_h) + \ldots. \end{aligned} \tag{4}$$

The first term on the right-hand side of Eq. (4) represents the steady-state heat flux q_{ss}, which reduces to its usual value $q_{ss} \to k(T_h - T_c)/l$ for a temperature-independent thermal conductivity ($k =$ constant), as expected. When k does depend on temperature, on the other hand, the periodic excitation $\Delta T\cos(\omega t)$ generates an additional net contribution that increases with the temperature derivatives of odd order of $k(T_h)$ and even powers of ΔT, as established by Eq. (4). This thermal-wave heat flux appears even in the absence of the steady-state one ($T_h = T_c = T$) and its leading contribution is driven by the slope of $k(T)$. In this case ($q_{ss} = 0$), the relation $\bar{q}l \approx k'(T)\,(\Delta T/2)^2$, for an approximation up to $(\Delta T/T)^3$, provides an effective way to control the intensity and direction of the net heat flux. If the thermal conductivity increases with temperature ($k'(T) > 0$), the thermal-wave heat flux propagates from the thermal bath with a modulated temperature to that with a steady-state temperature, reversing its direction for $k'(T) < 0$. The sign of $k'(T)$ thus drives the direction of the modulated heat flux, which disappears for any temperature satisfying the relation $k'(T) = 0$. As the thermal conductivity of most materials depends on temperature, this net heat flux of thermal waves is expected to appear and disappear in practically any solid material, even in the absence of a mean temperature gradient, and is analogous to the enhanced thermal convection observed in fluids subjected to temporally oscillating temperatures [3,44].

According to the mean value theorem applied to the integral in Eq. (2), the effective thermal conductivity of the material exposed to a dynamical temperature difference is given by

$$k_{\text{eff}} = \frac{ql}{T_h - T_c + \Delta T\cos(\omega t)}. \tag{5}$$

The values of k_{eff} thus exhibit a strong nonlinear dependence on time due to the oscillations of its numerator and denominator. After inserting Eq. (3) into Eq. (5) and expanding its denominator in powers of $\Delta T/(T_h - T_c)$, one obtains the following average of k_{eff} over one period $\tau = 2\pi/\omega$:

$$\bar{k}_{\text{eff}} = \frac{\bar{q}l}{U} - \frac{1}{2}\left(\frac{\Delta T}{U}\right)^2\left[k(T_h) + \left(\frac{\Delta T}{2\sqrt{2}}\right)^2 k''(T_h)\right] + \ldots, \tag{6}$$

where the average heat flux $\bar{q}$ is defined in Eq. (4) and we assumed that $\Delta T \ll U = T_h - T_c$. For a linear approximation on $\Delta T/U$, Eqs. (4) and (6) predict that the average heat flux and average effective thermal conductivity are related by Fourier's law $\bar{q} = \bar{k}_{\text{eff}}\,(T_h - T_c)\,/l$, as is the case for their temporal counterparts in Eq. (5). On the other hand, for an approximation up to $(\Delta T/U)^2$, the values of $\bar{k}_{\text{eff}}$ are driven not only by $\bar{q}$ but also by k and its second-order temperature derivative, due to the propagation of thermal waves. The thermal response of the material is therefore determined by the coupling of the steady-state and modulated effects, such that its effective thermal conductivity can be higher and lower than its steady-state counterpart $\bar{k}$, depending on ρ and $k'(T_h)$. For $T_h = T_c = T$, on the other hand, Eqs. (3) and (5) establish that the effective thermal conductivity is given by

$$\bar{k}_{\text{eff}} = k(T) + \frac{\Delta T^2}{12}k''(T) + \ldots. \tag{7}$$

In contrast to the average heat flux $\bar{q}$, the contribution of the thermal waves to $\bar{k}_{\text{eff}}$ is driven by the second-order temperature derivative of k. The dependence on k and k'' arises from the definition of $k_{\text{eff}} = ql/[\Delta T \cos(\omega t)]$ in Eq. (5), which keeps the average contribution of k and k'', and cancels out that of k', for $T_h = T_c$. The difference between Eqs. (6) and (7) thus establishes that the material thermal response is driven by the temperature difference $T_h - T_c$. In any case ($T_h > T_c$ or $T_h = T_c$), the excitation and propagation of thermal waves are expected to increase or decrease the effective thermal conductivity of nonlinear materials. Therefore, these waves could be used as effective heat carriers to harvest or evacuate thermal energy via the environmental temperature fluctuations.

III. RESULTS

The thermal energy harvesting or evacuation in a dynamical system without and with a mean temperature gradient will now be quantified for a Si plate, a common dielectric with a thermal conductivity exhibiting a peak at 40 K, as shown in Fig. 1(b).

Figure 2 shows the time oscillations of the heat flux q, temperature difference $\delta T = \Delta T \cos(\omega t)$, and thermal conductivity driving the propagation of thermal waves in a Si plate, for three representative temperatures $T = T_h = T_c$ around the peak temperature of its thermal conductivity. Since there is no steady-state temperature difference and the average of δT vanishes, over one period $\tau = 2\pi/\omega$, q represents the heat flux of thermal waves only and hence oscillates around zero. These q oscillations, predicted by Eq. (2), are accurately confirmed by the numerical solution (points) of Eq. (1a) and follow those of δT. Both q and δT take positive values for $0 < \omega t < \pi/2$ and $3\pi/2 < \omega t < 2\pi$ (green zones), and negative ones for $\pi/2 < \omega t < 3\pi/2$ (yellow zone). The positive and negative values of q are thus determined by δT, while the shape of the temporal q profile is driven by that of the thermal conductivity. For $T < 40$ K [Fig. 2(a)], the temperature of the modulated thermal bath oscillates between $T - \Delta T = 5$ K and $T + \Delta T = 35$ K, for which the temperature derivative of k is positive and q exhibits asymmetric oscillations taking positive values higher than its negative ones (in magnitude). This asymmetry over one period generates a positive average heat flux ($\bar{q} > 0$) and hence it flows from the modulated thermal bath to that with a steady-state temperature [from left to right in Fig. 1(a)]. For $T = 40$ K [Fig. 2(b)], on the other hand, the q oscillations become symmetrical around zero and therefore their average vanishes ($\bar{q} = 0$). This symmetry is induced by that of k, whose temperature derivative takes positive and negative values for the modulated thermal bath temperatures from $T - \Delta T = 25$ K to 40 K and from 40 K to $T + \Delta T = 55$ K, respectively. By contrast, for $T > 40$ K [Fig. 2(c)], the temperature of the modulated thermal bath oscillates between $T - \Delta T = 45$ K and $T + \Delta T = 75$ K, for which the temperature derivative of k is negative and q exhibits asymmetric

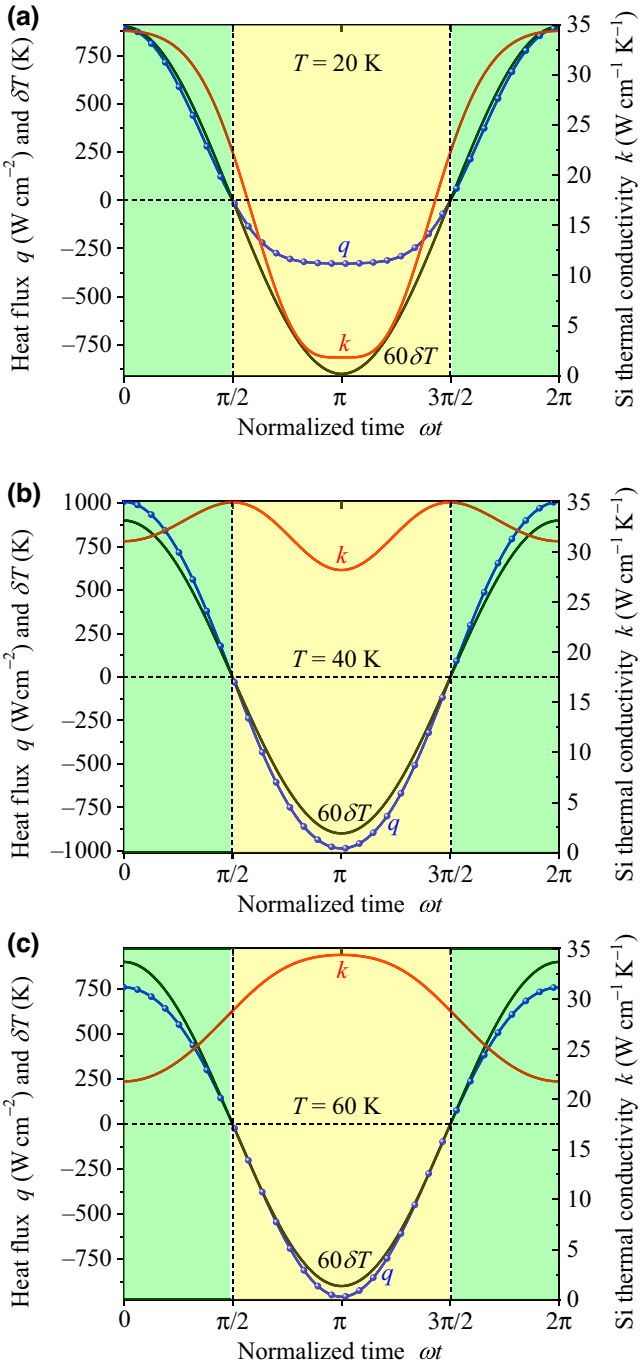

FIG. 2. Time evolution of the heat flux, temperature difference $\delta T = \Delta T \cos(\omega t)$, and Si thermal conductivity driving the heat conduction along a Si plate excited with $T_h = T_c = T$ and (a) $T = 20$ K, (b) $T = 40$ K, and (c) $T = 60$ K. The green and yellow zones represent positive and negative heat fluxes, respectively. Calculations were done for $l = 5$ mm, $\omega = 1$ rad/s and $\Delta T = 15$ K. Points represent the numerical predictions of finite-element method (FEM) simulations.

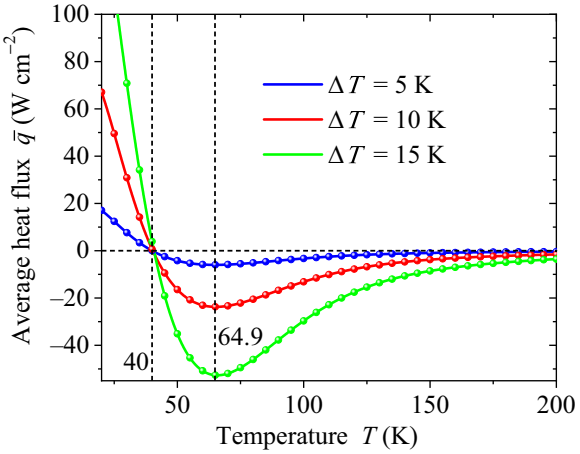

FIG. 3. Temperature evolution of the averaged heat flux in a Si plate subjected to $T = T_h = T_c$, $l = 5$ mm, and $\omega = 1$ rad/s. Points represent the predictions of FEM simulations.

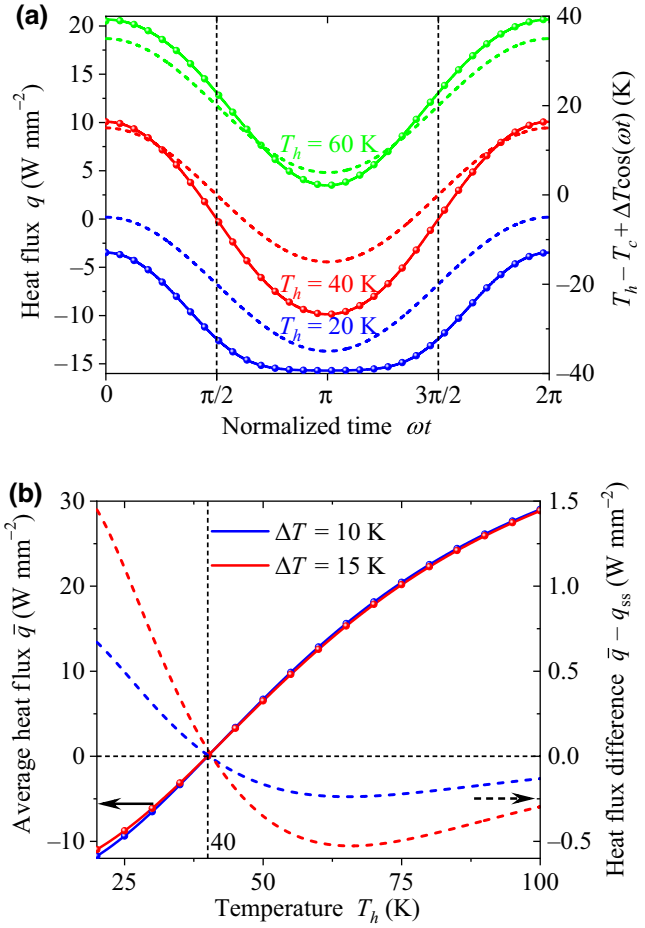

FIG. 4. (a) Time evolution of the heat flux and (b) its averaged counterpart as a function of temperature $T_h \neq T_c = 40$ K, for two amplitudes of the periodic excitation. The dashed lines in (a), (b) stand for the difference of temperature and heat flux specified in their right-hand-side vertical axes, respectively. Points represent the FEM numerical predictions. Calculations were done for $l = 5$ mm, $\omega = 1$ rad/s, and $\Delta T = 15$ K in (a).

oscillations dominated by negative values. Therefore, the average of q is expected to be negative ($\bar{q} < 0$) and flows from the thermal bath with constant temperature to that with a modulated one [from right to left in Fig. 1(a)].

The average heat flux $\bar{q}$ of thermal waves propagating along a Si plate is shown in Fig. 3 as a function of the temperature $T = T_h = T_c$. The analytical predictions (solid lines) of Eq. (4) are in very good agreement with the numerical ones (points) predicted by the finite-element method implemented in Comsol Multiphysics 6.2. Note that $\bar{q}$ increases with ΔT and vanishes at the Si peak temperature of 40 K, for the three values of ΔT. According to Fig. 1(b), this disappearance of the net heat flux arises from the vanishing temperature derivative of the thermal conductivity ($k'(T) = 0$ for $T = 40$ K), as predicted by Eq. (4). Further, $\bar{q}$ takes positive and negative values for $T < 40$ K ($k'(T) > 0$) and $T > 40$ K ($k'(T) < 0$), respectively. This behavior of $\bar{q}$ indicates that the approximation $\bar{q}l \approx k'(T)\,(\Delta T/2)^2$ of Eq. (4) is sufficiently accurate for the three relatively small values of the temperature amplitude ΔT. Further, the negative minimum of $\bar{q}$ at $T = 64.9$ K is generated by the dip of $k'(T)$ shown in Fig. 1(b). The Si plate excited with a temperature difference periodically modulated in time can thus be used as a modulator of the intensity and direction of the net heat flux of thermal waves.

In presence of a temperature difference $U = T_h - T_c \neq 0$, the heat conduction in the Si plate is driven not only by thermal waves, but also by the standard steady-state diffusion, as predicted by Eq. (3). The heat flux q and its average $\bar{q}$ over one period are shown in Fig. 4 as functions of time and temperature $T_h \neq T_c = 40$ K. In contrast to the heat flux obtained for $T_h = T_c = T$ [see Fig. 2 and the red line in Fig. 4(a)], q only oscillates through negative or positive values, for $T_h = 20$ K ($U = -20$ K) and $T_h = 60$ K ($U = +20$ K), respectively. The direction of q is thus mainly determined by the sign of the steady-state temperate difference U, while its time evolution is asymmetric with respect to the temperature difference oscillations (dashed lines) that generate it. This asymmetry results from the nonlinear dependence of q on $T_h - T_c + \Delta T\cos(\omega t)$ [see Eq. (2)] and yields an average heat flux that increases monotonically with T_h, as shown in Fig. 4(b). The magnitude of $\bar{q}$ also increases with $|U|$, but it is nearly independent of the modulation amplitude ΔT. This fact indicates that the values of $\bar{q}$ are driven by its steady-state component (q_{ss}), as confirmed by the heat flux difference $\bar{q} - q_{ss}$ (dashed lines), which is about one order of magnitude smaller than $\bar{q}$, for a given T_h. Therefore, the thermal waves do not contribute significantly to the heat conduction in a Si plate excited with relatively small values

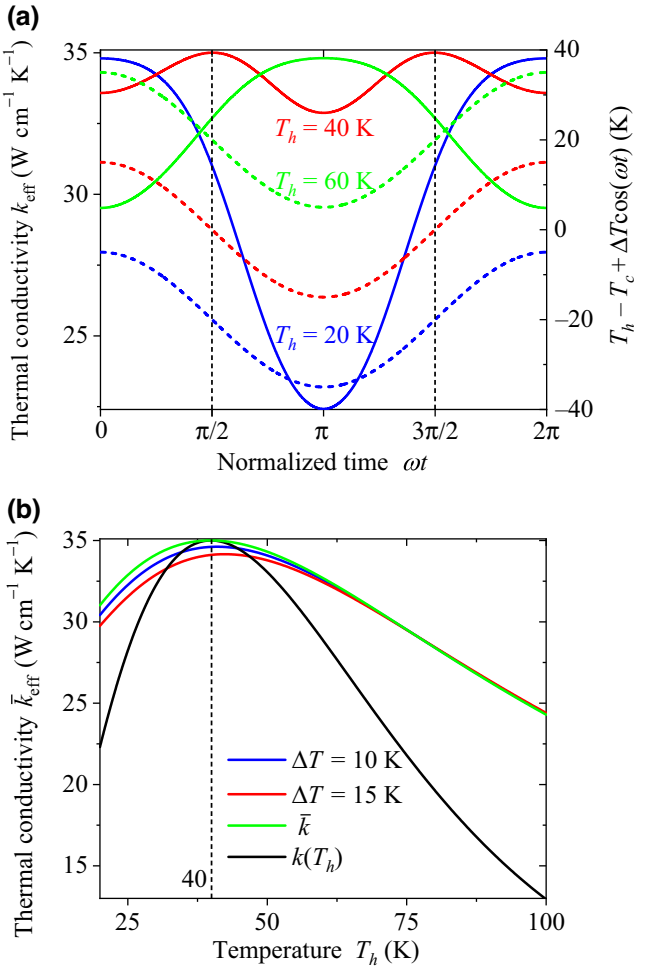

FIG. 5. (a) Time evolution of the effective thermal conductivity and (b) its averaged counterpart as a function of temperature $T_h > T_c = 40$ K, for two amplitudes of the periodic excitation. The dashed lines in (a) stand for the temperature difference specified in its right-hand-side vertical axes, while the black line in (b) represents the Si thermal conductivity. Calculations were done for $l = 5$ mm and $\omega = 1$ rad/s.

of $\Delta T \leq 15$ K. However, higher thermal-wave heat fluxes are expected for larger modulation amplitudes.

The asymmetry of the heat flux variation with time is also exhibited by the effective thermal conductivity $k_{\rm eff}$, as shown in Fig. 5(a). For $T_h = 20$ K, $k_{\rm eff}$ opens upward and changes significantly over one period of time. These changes reduce for $T_h = 60$ K, for which $k_{\rm eff}$ opens downward. By contrast, for $T_h = 40$ K, the oscillations of $k_{\rm eff}$ shrink through values that are relatively higher than those obtained for $T_h = 20$ and 60 K. This fact indicates that the average effective thermal conductivity $\bar{k}_{\rm eff}$ is expected to take its maximum at the peak temperature (40 K) of the Si thermal conductivity, as confirmed by Fig. 5(b). For a given temperature in the vicinity of $T_h = 40$ K, the values of $\bar{k}_{\rm eff}$ are smaller than its corresponding steady-state counterpart $\bar{k}$. The relatively small increase of the thermal conductivity difference $\bar{k} - \bar{k}_{\rm eff}$ with the modulation amplitude ΔT is consistent with the heat flux behavior shown in Fig. 4(b) and could be enhanced for $\Delta T > 15$ K.

IV. DISCUSSION

Assuming that the Si plate separates an outdoor environment (left thermal bath) from an indoor one (right thermal bath) at nearly the same mean temperature, the proposed heat modulator could be used to harvest or evacuate thermal energy via the outdoor temperature fluctuations. If the environment is at low temperature ($T < 40$ K), the net heat flux flows from outdoors to indoors and hence the modulator harvests thermal energy. By contrast, if the environment is at high temperature ($T > 40$ K), the net heat flux flows from indoors to outdoors and therefore the modulator evacuates thermal energy. As the outer space temperature may fluctuate in the vicinity of the peak temperature (40 K) of the Si thermal conductivity, the Si plate could be used as a harvester or evacuator of thermal energy in spatial missions close to the edges of our solar system. The proposed heat flux modulator could, of course, also be applied on earth; however, its operation requires the development of materials with a thermal conductivity peak close to 300 K. These materials could be based on $(Pb_{1-x}Sn_x)Se$, a solid made up of cubic lead selenide (PbSe) and layered tin selenide (SnSe), whose thermal conductivity exhibits a peak at 373 K [45].

The fact that both $\bar{k}_{\rm eff}$ and $\bar{k}$ are significantly higher than the Si thermal conductivity [Fig. 5(b)], for temperatures outside the neighborhood of $T_h = T_c = 40$ K, shows that silicon becomes a better thermal conductor, when exposed to large temperature gradients, as predicted by Eq. (6). The steady-state temperature difference $T_h - T_c$ and the modulation amplitude ΔT thus represent two degrees of freedom to modulate the effective thermal conductivity and total heat flux in silicon. This modulation of key thermal parameters could also be obtained with other materials whose thermal conductivity significantly changes with temperature. As these changes are typically present for temperatures around the thermal conductivity peak of dielectrics, the proposed thermal modulation paves the way to harvesting or evacuating heat through temperature fluctuations propagating in a great variety of materials.

The net heat flux of thermal waves could be measured by placing a Si plate between two Peltier cells, which typically control temperatures with a resolution better than 0.1 K and modulation frequencies from 0.1 to 100 Hz [46]. The modulated temperature of the left-hand-side surface of the Si plate can be set with a Peltier cell, while its right-hand-side surface is kept at constant temperature with a second Peltier cell. The heat flux in the cell–Si–cell system could then be recorded through a heat flux sensor in contact with the left-hand-side Peltier cell, as was experimentally done for other systems [47].

Although this work is limited to quantifying the net heat flux of thermal waves for a sinusoidal thermal excitation only, we anticipate that this thermal energy could also be harvested or evacuated for an external temperature excitation with an arbitrary dependence on time. By expressing this latter excitation as a superposition of sines and cosines via its Fourier series, Fourier's law establishes that the average heat flux of thermal waves is still driven by the temperature derivative of the thermal conductivity, as shown in our previous work [11]. Further, the harvesting or evacuation of the thermal-wave heat currents is also expected to be present for non-quasisteady-state regimes, for which the heat capacity effects become important. These high-frequency effects will generally change the spatial distribution of the temperature profile (for $T_h \neq T_c$) and therefore the net heat flux of thermal waves will be driven not only by the temperature dependence of the thermal conductivity, but also by that of heat capacity, as established by Fourier's law of heat conduction.

V. CONCLUSIONS

We have demonstrated the existence of a net heat flux driven by the nonlinear propagation of thermal diffusion waves in a material with a periodically oscillating temperature. This thermal-wave heat flux is determined by the temperature derivative of the material thermal conductivity and exists even in the absence of an average temperature difference. In the presence of a net temperature difference, this heat flux amplifies or weakens its steady-state counterpart depending on the positive or negative sign of the thermal conductivity slope, respectively. The total heat flux can thus be tuned by adjusting the material's temperature around its thermal conductivity peak, common in dielectrics. Further, we have found that the heat flux increases proportionally to the square of the excitation temperature amplitude. This finding is expected to facilitate the observation and application of the thermal-wave heat flux to harvest and dissipate energy in systems experiencing temperature fluctuations.

[1] A. Mandelis, Diffusion waves and their uses, Phys. Today **53**, 29 (2000).

[2] D. Almond and P. Patel, *Photothermal Science and Techniques* (Springer, London, 1996).

[3] P. Urban, P. Hanzelka, T. Králik, V. Musilová, and L. Skrbek, Thermal waves and heat transfer efficiency enhancement in harmonically modulated turbulent thermal convection, Phys. Rev. Lett. **128**, 134502 (2022).

[4] C. L. Gomez-Heredia, J. A. Ramirez-Rincon, J. Ordonez-Miranda, O. Ares, J. J. Alvarado-Gil, C. Champeaux, F. Dumas-Bouchiat, Y. Ezzahri, and K. Joulain, Thermal hysteresis measurement of the VO_2 emissivity and its application in thermal rectification, Sci. Rep. **8**, 8479 (2018).

[5] J. Ordonez-Miranda, L. Jalabert, Y. Wu, S. Volz, and M. Nomura, Analytical integration of the heater and sensor 3ω signals of anisotropic bulk materials and thin films, J. Appl. Phys. **133**, 205104 (2023).

[6] F. Yang, Z. Zhang, L. Xu, Z. Liu, P. Jin, P. Zhuang, M. Lei, J. Liu, J.-H. Jiang, X. Ouyang, F. Marchesoni, and J. Huang, Controlling mass and energy diffusion with metamaterials, Rev. Mod. Phys. **96**, 015002 (2024).

[7] Z. Zhang, L. Xu, T. Qu, M. Lei, Z.-K. Lin, X. Ouyang, J.-H. Jiang, and J. Huang, Diffusion metamaterials, Nat. Rev. Phys. **5**, 218 (2023).

[8] P. Zhuang, X. Zhou, L. Xu, and J. Huang, Cooperative near- and far-field thermal management via diffusive superimposed dipoles, Appl. Phys. Rev. **11**, 011416 (2024).

[9] E. Marín, J. Marín-Antuña, and P. Díaz-Arencibia, On the wave treatment of the conduction of heat in photothermal experiments with solids, Eur. J. Phys. **23**, 523 (2002).

[10] A. Salazar, Energy propagation of thermal waves, Eur. J. Phys. **27**, 1349 (2006).

[11] J. Ordonez-Miranda, R. Anufriev, M. Nomura, and S. Volz, Net heat current at zero mean temperature gradient, Phys. Rev. B **106**, L100102 (2022).

[12] P. Jin, J. Liu, L. Xu, J. Wang, X. Ouyang, J.-H. Jiang, and J. Huang, Tunable liquid–solid hybrid thermal metamaterials with a topology transition, Proc. Natl. Acad. Sci. **120**, e2217068120 (2023).

[13] P. Jin, L. Xu, G. Xu, J. Li, C.-W. Qiu, and J. Huang, Deep learning-assisted active metamaterials with heat-enhanced thermal transport, Adv. Mater. **36**, 2305791 (2024).

[14] L. Xu, G. Xu, J. Li, Y. Li, J. Huang, and C.-W. Qiu, Thermal willis coupling in spatiotemporal diffusive metamaterials, Phys. Rev. Lett. **129**, 155901 (2022).

[15] L. L. N. Laboratory, Energy flow charts: Charting the complex relationships among energy, water, and carbon (2024), https://flowcharts.llnl.gov.

[16] J. Ordonez-Miranda, Radiative thermostat driven by the combined dynamics of electrons, phonons, and photons, Phys. Rev. Appl. **14**, 064043 (2020).

[17] B. Li, L. Wang, and G. Casati, Thermal diode: Rectification of heat flux, Phys. Rev. Lett. **93**, 184301 (2004).

[18] M. Terraneo, M. Peyrard, and G. Casati, Controlling the energy flow in nonlinear lattices: A model for a thermal rectifier, Phys. Rev. Lett. **88**, 094302 (2002).

[19] J. Hu, X. Ruan, and Y. P. Chen, Thermal conductivity and thermal rectification in graphene nanoribbons: A molecular dynamics study, Nano Lett. **9**, 2730 (2009).

[20] J. Ordonez-Miranda, J. M. Hill, K. Joulain, Y. Ezzahri, and J. Drevillon, Conductive thermal diode based on the thermal hysteresis of VO_2 and nitinol, J. Appl. Phys. **123**, 085102 (2018).

[21] A. Fornieri, M. J. Martinez-Perez, and F. Giazotto, A normal metal tunnel-junction heat diode, Appl. Phys. Lett. **104**, 183108 (2014).

[22] B. Li, L. Wang, and G. Casati, Negative differential thermal resistance and thermal transistor, Appl. Phys. Lett. **88**, 143501 (2006).

[23] N. Li, J. Ren, L. Wang, G. Zhang, P. Hanggi, and B. Li, Phononics: Manipulating heat flow with electronic analogs and beyond, Rev. Mod. Phys. **84**, 1045 (2012).

[24] L. Wang and B. Li, Thermal logic gates: Computation with phonons, Phys. Rev. Lett. **99**, 177208 (2007).

[25] L. Wang and B. Li, Thermal memory: A storage of phononic information, Phys. Rev. Lett. **101**, 267203 (2008).
[26] P. Ben-Abdallah, Thermal memristor and neuromorphic networks for manipulating heat flow, AIP Adv. **7**, 065002 (2017).
[27] F. Yang, M. P. Gordon, and J. J. Urban, Theoretical framework of the thermal memristor via a solid-state phase change material, J. Appl. Phys. **125**, 025109 (2019).
[28] X. Shen, Y. Li, C. Jiang, and J. Huang, Temperature trapping: Energy-free maintenance of constant temperatures as ambient temperature gradients change, Phys. Rev. Lett. **117**, 055501 (2016).
[29] J. Wang, J. Shang, and J. Huang, Negative energy consumption of thermostats at ambient temperature: Electricity generation with zero energy maintenance, Phys. Rev. Appl. **11**, 024053 (2019).
[30] J. Ordonez-Miranda, Y. Ezzahri, J. Drevillon, and K. Joulain, Dynamical heat transport amplification in a far-field thermal transistor of VO_2 excited with a laser of modulated intensity, J. Appl. Phys. **119**, 203105 (2016).
[31] K. Ito, K. Nishikawa, A. Miura, H. Toshiyoshi, and H. Iizuka, Dynamic modulation of radiative heat transfer beyond the blackbody limit, Nano Lett. **17**, 4347 (2017).
[32] I. Latella, R. Messina, J. M. Rubi, and P. Ben-Abdallah, Radiative heat shuttling, Phys. Rev. Lett. **121**, 023903 (2018).
[33] J. Ren and B. Li, Emergence and control of heat current from strict zero thermal bias, Phys. Rev. E **81**, 021111 (2010).
[34] N. Li, F. Zhan, P. Hänggi, and B. Li, Shuttling heat across one-dimensional homogenous nonlinear lattices with a Brownian heat motor, Phys. Rev. E **80**, 011125 (2009).
[35] N. Li, P. Hanggi, and B. Li, Ratcheting heat flux against a thermal bias, EPL **84**, 40009 (2008).
[36] Q. Liu and M. Xiao, Energy harvesting from thermal variation with phase-change materials, Phys. Rev. Appl. **18**, 034049 (2022).
[37] J.-C. Krapez, Influence of thermal hysteresis on the heat shuttling effect: The case of VO_2, J. Appl. Phys. **133**, 195102 (2023).
[38] J. Li, Y. Li, P.-C. Cao, M. Qi, X. Zheng, Y.-G. Peng, B. Li, X.-F. Zhu, A. Alù, H. Chen, and C.-W. Qiu, Reciprocity of thermal diffusion in time-modulated systems, Nat. Commun. **13**, 167 (2022).
[39] G. Xu, Y. Li, W. Li, S. Fan, and C.-W. Qiu, Configurable phase transitions in a topological thermal material, Phys. Rev. Lett. **127**, 105901 (2021).
[40] J. Ordonez-Miranda, Y. Guo, J. J. Alvarado-Gil, S. Volz, and M. Nomura, Thermal-wave diode, Phys. Rev. Appl. **16**, L041002 (2021).
[41] C. J. Glassbrenner and G. A. Slack, Thermal conductivity of silicon and germanium from 3 K to the melting point, Phys. Rev. **134**, A1058 (1964).
[42] J. Yoon, H. Kim, X. Chen, N. Tamura, B. S. Mun, C. Park, and H. Ju, Controlling the temperature and speed of the phase transition of VO_2 microcrystals, ACS Appl. Mater. Interfaces **8**, 2280 (2016).
[43] A. J. L. P. Flubacher and J. A. Morrison, The heat capacity of pure silicon and germanium and properties of their vibrational frequency spectra, Philos. Mag.: J. Theor. Exp. Appl. Phys. **4**, 273 (1959).
[44] R. Yang, K. L. Chong, Q. Wang, R. Verzicco, O. Shishkina, and D. Lohse, Periodically modulated thermal convection, Phys. Rev. Lett. **125**, 154502 (2020).
[45] Y. Nishimura, X. He, T. Katase, T. Tadano, K. Ide, S. Kitani, K. Hanzawa, S. Ueda, H. Hiramatsu, H. Kawaji, H. Hosono, and T. Kamiya, Electronic and lattice thermal conductivity switching by 3D-2D crystal structure transition in nonequilibrium $(Pb_{1-x}Sn_x)Se$, Adv. Electron. Mater. **8**, 2200024 (2022).
[46] F. Cervantes-Alvarez, J. D. Macias, and J. J. Alvarado-Gil, Heat transport in electrically aligned multiwalled carbon nanotubes dispersed in water, J. Phys. D **51**, 065302 (2018).
[47] I. Forero-Sandoval, J. Chan-Espinoza, J. Ordonez-Miranda, J. Alvarado-Gil, F. Dumas-Bouchiat, C. Champeaux, K. Joulain, Y. Ezzahri, J. Drevillon, C. Gomez-Heredia, and J. Ramirez-Rincon, VO_2 substrate effect on the thermal rectification of a far-field radiative diode, Phys. Rev. Appl. **14**, 034023 (2020).